ADVANCES IN ATMOSPHERIC SCIENCES, VOL. 32, JUNE 2015, 870–876

# Dryland Expansion in Northern China from 1948 to 2008

LI Yue, HUANG Jianping*, JI Mingxia, and RAN Jinjiang

*Key Laboratory for Semi-Arid Climate Change of the Ministry of Education, College of Atmospheric Sciences, Lanzhou University, Lanzhou* 730000

(Received 17 May 2014; revised 17 October 2014; accepted 29 October 2014)

ABSTRACT

This study examines the expansion of drylands and regional climate change in northern China by analyzing the variations in aridity index (AI), surface air temperature (SAT), precipitation and potential evapotranspiration (PET) from 1948 to 2008. It is found that the drylands of northern China have expanded remarkably in the last 61 years. The area of drylands of the last 15 years (1994–2008) is $0.65 \times 10^6$ km$^2$ (12%) larger than that in the period 1948–62. The boundary of drylands has extended eastward over Northeast China by about 2° of longitude and by about 1° of latitude to the south along the middle-to-lower reaches of the Yellow River. A zonal band of expansion of semi-arid regions has occurred, stretching from western Heilongjiang Province to southern Gansu Province, while shifts to the east of semi-arid regions in dry subhumid regions have also occurred. Results show that the aridity trend of drylands in northern China is highly correlated with the long-term trend of precipitation and PET, and the expansion of semi-arid regions plays a dominant role in the areal extent of drylands, which is nearly 10 times larger than that in arid and subhumid regions.

**Key words**: aridity index, dryland expansion, climate variation, northern China

**Citation**: Li, Y., J. P. Huang, M. X. Ji, and J. J. Ran, 2015: Dryland expansion in northern China from 1948 to 2008. *Adv. Atmos. Sci.*, **32**(6), 870–876, doi: 10.1007/s00376-014-4106-3.

## 1. Introduction

Drylands are areas where precipitation is scarce and typically unpredictable, and can be divided into four subtypes: hyper-arid, arid, semi-arid, and dry subhumid areas. Drylands cover about 41% of Earth's land surface, are home to about 35% of the world's population, and have some of the highest levels of poverty (GLP, 2005; Millennium Ecosystem Assessment, 2005; Mortimore, 2009). Drylands are characterized by a dry climate and a low nutrition content and water conservation capacity of soil. The ecosystems of drylands are vulnerable and sensitive to climate change and human activities (Dietz et al., 2004; Reynolds et al., 2007; Reed et al., 2012). Feng and Fu (2013) showed that global drylands have expanded in the last 60 years, and will continue to expand in the 21st century. Expansions of drylands have a direct consequence for desertification, defined as land degradation in arid, semi-arid and dry subhumid areas resulting from various factors, including climatic variations and human activities [United Nations Convention to Combat Desertification (UNCCD), 1994]. Some form of severe land degradation is present in 10%–20% of drylands, a figure that is likely to expand substantially in the face of climate change and population growth (Reynolds et al., 2007). In drylands, the combination of climatic variability and imprudent land use can adversely alter the region's climate (Nicholson, 2011).

Recent research has revealed that drying trends over drylands under global warming can be detected from both observations and model simulations (Ma and Fu, 2006, 2007; Fu et al., 2008; Overpeck and Udall, 2010; Dai, 2013), and increases in the extent and severity of desertification or degradation, which can be attributed to both climate change and human activities (Sun, 2000; Wang et al., 2003; Yang et al., 2005; Wang et al., 2006). An important consequence of the expansion of drylands is desertification, which is a central issue for sustainable development (Reynolds et al., 2007). Moreover, the loss of vegetation cover may exacerbate the impacts of drought, and increased aridity will promote the mobilization of dust, further leading to frequent dust storms originating from dust source regions (Wang et al., 2008). The effect of dust aerosols on climate over drylands will become more evident (Huang et al., 2010; Xi and Sokolik, 2012; Huang, 2013). Therefore, research has been conducted on the impact of dust aerosols on climate in northern China by using satellite observations (Huang et al., 2007, 2010; Chen et al., 2010), ground-based measurements (Huang et al., 2008; Wang et al., 2010; Bi et al., 2011; Wang et al., 2013b, 2014), and model simulations (Chen et al., 2013).

As we know, climatic fluctuations and human mismanagement could initiate the process of desertification and even a long-term degradation of the environment. Knowledge of

* Corresponding author: HUANG Jianping
Email: hjp@lzu.edu.cn

how climate change and human activities will affect the extent of drylands is essential for the protection and proper management of these regions, in order to maintain drylands as sustainable resources (Reynolds et al., 2007; Mortimore, 2009; Nicholson, 2011). Although globally drylands have already been investigated by many studies (e.g. Hulme, 1996; Seager et al., 2007; Feng and Fu, 2013), only a few studies have focused on the regional climate of drylands in East Asia, especially northern China. For example, Ma and Fu (2003) and Ma and Dan (2005) studied climate change over drylands in northern China, demonstrating that the aridity trend has been further aggravated. Aridification has intensified over Northeast China due to regional climate changes related to global warming as well as the anthropogenic effects of the rapid development of the social economy and the expansion of urbanization (Fu et al., 2008). The subsequent expansion of drylands will cause an increase in the population affected by water scarcity and land degradation.

In this paper, we examine the expansion of drylands in northern China and the regional climate variability over drylands by analyzing datasets of aridity index, surface air temperature, precipitation, and potential evapotranspiration from 1948 to 2008, and try to explain the possible reasons for the expansion. The methods and data used in this study are described in section 2, and results regarding dryland expansion and climate change over drylands are presented in sections 3 and 4, respectively. Further discussion and a summary are provided in section 5.

## 2. Methods and data

### 2.1. *Aridity indices*

Aridity refers to the dryness of the atmosphere, which is essentially a climatic phenomenon that is based on average climatic conditions over a region (Agnew and Anderson, 1992). Numerous numerical indices have been proposed to quantify the degree of climatic dryness at a given location [see the review of aridity indices by Stadler (2005)]. However, there is a lack of agreement over the approaches used to delineate the exact boundaries between lands of differing aridity.

The simplest aridity index is based solely on precipitation. A commonly used rainfall-based definition is that drylands receive less than 600 mm of precipitation per year, and can be further divided into hyper-arid (annual precipitation $\leqslant$50 mm), arid (50 mm$<$annual precipitation $\leqslant$200 mm), semi-arid (200 mm $<$ annual precipitation $\leqslant$400 mm), and dry subhumid (400 mm$<$annual precipitation $\leqslant$600 mm) regions.

Aridity index (AI) is defined as the ratio of annual precipitation to annual potential evapotranspiration (PET), which is a quantitative indicator of the degree of water deficiency at a given location. Drylands are regions with AI $\leqslant$0.65, which are further divided into hyper-arid (AI $\leqslant$0.05), arid (0.05$<$AI$\leqslant$0.2), semi-arid (0.2$<$AI$\leqslant$0.5), and dry subhumid (or subhumid for simplicity) (0.5$<$AI$\leqslant$0.65) regions (Middleton and Thomas, 1997; Mortimore, 2009). PET represents the evaporative demand of the atmosphere. It is calculated by the Penman–Monteith algorithm (Maidment, 1993), which includes the effects of temperature, humidity, solar radiation and wind. This algorithm is superior to other formulations, which usually only consider the effect of temperature (Donohue et al., 2010; Dai, 2011; Feng and Fu, 2013).

### 2.2. *Data*

The monthly mean surface air temperature (SAT) and precipitation datasets from 1948 to 2008 developed by the Climate Prediction Center (CPC) are used in this study (Chen et al., 2002; Fan and van den Dool, 2008). The datasets are globally gridded at $0.5^\circ \times 0.5^\circ$ resolution. To calculate PET using the Penman–Monteith algorithm, SAT, specific humidity, solar radiation and wind speed are needed. Owing to the scarcity of observations for specific humidity, solar radiation and wind speed, the datasets of these quantities are from the Global Land Data Assimilation System (GLDAS) (Rodell et al., 2004) starting from 1948. The resolution of the data is $0.5^\circ \times 0.5^\circ$. The data of global surface vegetation types are from satellite Moderate Resolution Imaging Spectroradiometer (MODIS) observations [ISLSCP II MODIS (Collection 4, 2010) IGBP Land Cover].

## 3. Results

### 3.1. *Expansion of drylands in northern China*

The distribution of drylands, including the individual components in northern China for 1961–90 climatology, as identified by the two considered definitions of AI and annual precipitation, are shown in Figs. 1a and b. The area of dryland defined by AI (Fig. 1a) is smaller than that defined by annual precipitation (Fig. 1b). The hyper-arid and arid regions match well, and the main differences are over semi-arid and subhumid regions. In northeastern Inner Mongolia and most of Heilongjiang, the classification is subhumid based on annual precipitation, while it is humid based on AI. Aridity is a function of the interplay between temperature, precipitation and evaporation. The use of annual precipitation as an index of aridity ignores the importance of temperature and evaporation; therefore, the classification of drylands based on AI is more reasonable and reliable, and is used in the following analyses.

As shown in Fig. 1a, semi-arid regions dominate the coverage of drylands, which are distributed in a northeast–northwest zonal band, covering most of Inner Mongolia, Hebei, northern Shaanxi, Ningxia, central Gansu, Qinghai and Tibet. There are also some small areas over Junggar Basin and Tianshan Mountains. The total area of semi-arid regions is $2.14 \times 10^6$ km$^2$, and these regions are mainly covered by grassland (Fig. 1c). The hyper-arid regions mainly occur in Northwest China, mostly covering Xinjiang Province, some parts of Gansu, Qinghai and Tibet, and the northwestern edge of Inner Mongolia. The arid regions surround the hyper-arid regions and extend eastward to central Inner Mongolia.

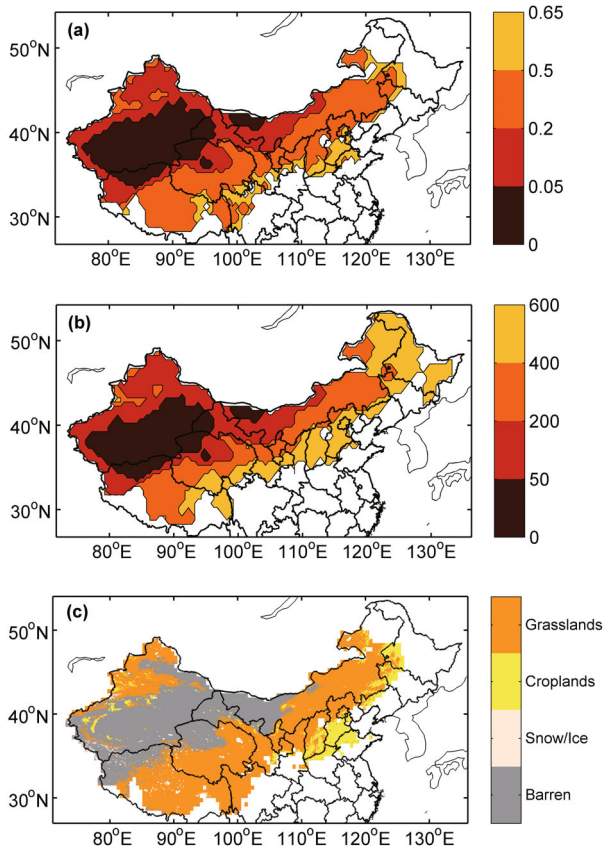


**Fig. 1.** Distribution of drylands in northern China for 1961–90 climatology based on (a) AI and (b) annual precipitation (mm) versus (c) corresponding surface vegetation types from MODIS observations.

The hyper-arid and arid regions are dominated by barren or sparsely vegetated land. Moreover, the dry subhumid regions only distribute in a narrow band along the southern edge of the semi-arid regions, where the MODIS surface vegetation types are grassland and cropland (Liu et al., 2013a). The areas of hyper-arid, arid and dry subhumid regions are $1.06 \times 10^6$, $1.42 \times 10^6$ and $1.00 \times 10^6$ km$^2$, respectively. Hence, the total area of drylands is $5.62 \times 10^6$ km$^2$ in northern China. The derived spatial distribution of drylands (Fig. 1a) generally matches well with the surface vegetation types over those regions from MODIS observations (Fig. 1c). However, there is no exact match between the dryland subtypes and the surface vegetation types. For example, barren and grassland may occur in different areas of the same dryland subtype (i.e. arid); grassland even occurs in three different dryland subtypes of arid, semi-arid and subhumid regions. The presence of different surface vegetation types in each dryland subtype demonstrates that vegetation species respond not only to the overall moisture deficit but also to other environmental variables, such as soils, geomorphological and landscape features (Safriel and Adeel, 2005).

The temporal variations of dryland areas in northern China, including the total and individual components of hyper-arid, arid, semi-arid and dry subhumid regions are shown in Fig. 2. It can be seen that the drylands for the total and individual components over China have been expanding during the last 61 years, except for the hyper-arid regions. Among those components, the expansion of semi-arid regions is the fastest, by $0.111 \times 10^6$ km$^2$ (10 yr)$^{-1}$, which is about 10 times faster than those of arid and dry subhumid regions [$0.013 \times 10^6$ and $0.017 \times 10^6$ km$^2$ (10 yr)$^{-1}$, respectively]. However, the hyper-arid regions have shrunk slightly from 1948 to 2008, at a rate of change of $-0.002 \times 10^6$ km$^2$ (10 yr)$^{-1}$. In summary, the total dryland area has been expanding rapidly by $0.12 \times 10^6$ km$^2$ (10 yr)$^{-1}$, driven mainly by the rapid expansion of semi-arid regions.

We also compare the areas of drylands in northern China in the last 15 years (1994–2008) with those in the earliest 15 years of the time series of the datasets (1948–62). All the components of drylands expanded except for the hyper-arid regions, and the expansion of semi-arid regions in northern China is very significant. The drylands in northern China have increased in units of $10^6$ km$^2$ by 0.06 for arid, 0.63 for semi-arid, and 0.03 for dry subhumid regions, relative to 1948–62 (Table 1). These increases correspond to relative increases of 4%, 33% and 3%, respectively. Note that the expansion of semi-arid regions is the most severe during the last 61 years, which is more than 10 times larger than those in the other two regions. On the contrary, the area of hyper-arid regions has decreased by $0.07 \times 10^6$ km$^2$ (6%). The average area of all drylands of the last 15 years (1994–2008) is $6.07 \times 10^6$ km$^2$, which is $0.65 \times 10^6$ km$^2$ (12%) larger than that for 1948–62.

The boundaries of areal change of drylands from 1948–62 to 1994–2008 show that the expansion of drylands mainly occurs over Northeast China and the middle-to-lower reaches of the Yellow River (see Fig. 3). In Northeast China, drylands expanded eastward dramatically by about 2° of longitude, especially over the northwest of Inner Mongolia, and the area of expansion is almost equivalent to the entire area of Liaoning Province. A few patches in southern Heilongjiang Province

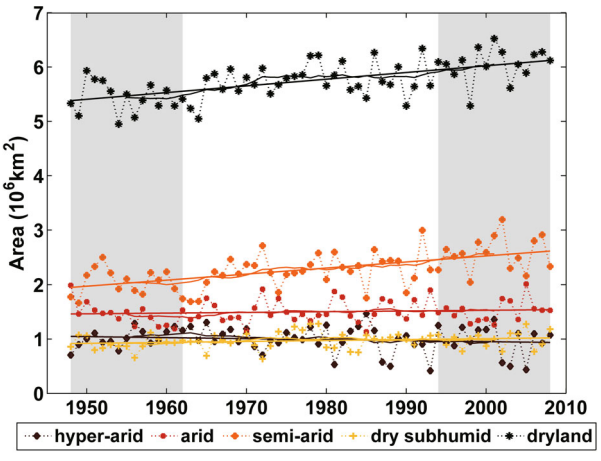


**Fig. 2.** Temporal variations in areal coverage of drylands in northern China for the total and individual components in units of $10^6$ km$^2$. Thick lines are 15-yr smoothed to emphasize the climate change. Solid lines are the fit to the data of the total and individual component of drylands.

**Table 1.** Areal changes of drylands in northern China for the total and individual components of hyper-arid, arid, semi-arid and dry subhumid regions from 1948–62 to 1994–2008, in units of $10^6$ km$^2$.

| | Area | | | | |
|---|---|---|---|---|---|
| | Hyper-arid | Arid | Semi-arid | Subhumid | Drylands |
| 1948–62 | 1.12 | 1.35 | 1.93 | 1.02 | 5.42 |
| 1994–2008 | 1.05 | 1.41 | 2.56 | 1.05 | 6.07 |
| Difference | −0.07 | 0.06 | 0.63 | 0.03 | 0.65 |
| Relative difference(%) | −6% | 4% | 33% | 3% | 12% |

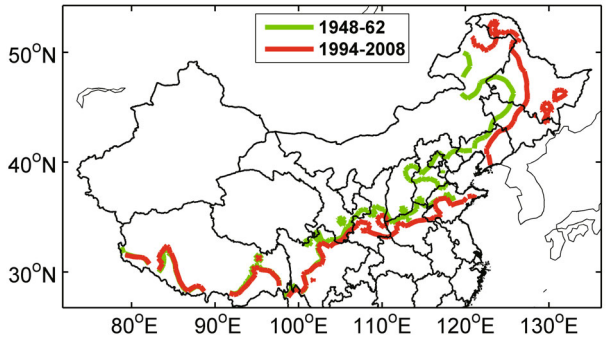


**Fig. 3.** The boundaries of areal change of drylands from 1948–62 (green) to 1994–2008 (red).

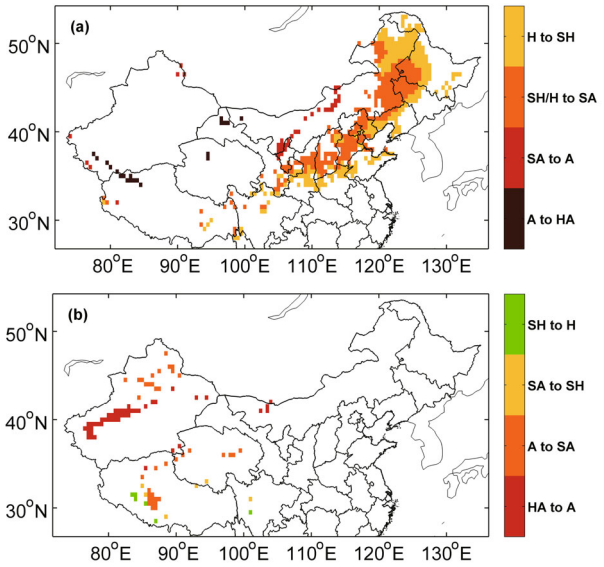


**Fig. 4.** Changes in coverage to (a) drier types and (b) wetter types for 1994–2008 relative to 1961–90. H, SH, SA, A, and HA represent humid, subhumid, semi-arid, arid and hyper-arid, respectively.

and Liaodong Peninsula turned into drylands in the last 15 years. In addition, over the middle-to-lower reaches of the Yellow River, drylands expanded southward by about 1° of latitude. In central Shaanxi Province in particular, the expansion reaches 2° of latitude. The Shandong Peninsula has also turned into dryland in the last 15 years. The southwestern boundary of drylands has remained relatively stationary, so the expansion is not obvious in the west between 1948–62 and 1994–2008. This result is consistent with a previous study by Ma et al. (2005), which shows that there is a trend of the boundaries moving eastward or southward in the last 100 years, and the trend is particularly pronounced for the arid and semi-arid boundaries during the last 50 years.

Figure 4a shows the changes in coverage to drier types for the last 15 years relative to 1961–90 climatology. It can be seen that the expansion of semi-arid regions occurs over Northeast China, which shows a zonal band stretching from western Heilongjiang, Jilin and eastern Inner Mongolia, across most of Hebei, Shanxi and Shaanxi, and then to southern Gansu. Major expansions of dry subhumid regions have also occurred over Northeast China, to the east of semi-arid regions, including western Heilongjiang, Jilin and Liaoning, and a large coverage in northeast Inner Mongolia. The expansions of arid and hyper-arid regions are relatively small and have mainly occurred in a narrow zonal band across central Inner Mongolia and on the western edge of the Kunlun mountains, respectively. The expansion of drylands is not a universal trend; some regions have experienced dryland retreat, suggesting they are getting wetter. As Fig. 4b shows, a retreat of hyper-arid to arid regions has occurred on the edges of the Tarim Basin and Tianshan Mountains, and a retreat of arid to semi-arid regions can be seen to have mainly occurred over central Tibet and in small patches on the edge of Junggar Basin. Moreover, the coverage of the retreat of semi-arid (subhumid) to subhumid (humid) is even smaller and scattered. It is clear that the areas with reduced aridity are much smaller than those with intensified aridity (Fig. 4b).

The total area of drylands has increased by $0.65 \times 10^6$ km$^2$ between 1948–62 and 1994–2008 (Table 1). The contributions of different type transitions to the areal change have been calculated (Table 2). The area of hyper-arid regions has reduced by $0.065 \times 10^6$ km$^2$. This change has two components, including the expansion of arid to hyper-arid regions ($0.049 \times 10^6$ km$^2$) and the retreat of hyper-arid to arid regions ($0.114 \times 10^6$ km$^2$). Hyper-arid is already the driest type, so it can only expand from and retreat to wetter type, which is arid. For the other components of drylands, four situations have to be taken into account, since both expansion and retreat have two transitions from/to drier and wetter types, respectively. For example, the areal change of semi-arid regions is $0.625 \times 10^6$ km$^2$ between 1948–62 and 1994–2008, calculated by considering two aspects. One aspect is the expansion of the two transitions from arid to semi-arid regions (from drier type, $0.092 \times 10^6$ km$^2$) and from subhumid/humid to semi-arid regions (from wetter type, $0.638 \times 10^6$ km$^2$); and the other is the retreat, which also includes two transitions from semi-arid to arid regions (to drier type, $0.084 \times 10^6$ km$^2$) and from semi-arid to subhumid regions (to wetter type, $0.021 \times 10^6$ km$^2$). The net expansion is then simply the total expansion minus the total retreat. It can be seen that the expansion of semi-arid regions is very severe, contributed mostly by the transitions from wetter type (i.e. subhumid/humid). Note that the areal change of the expansion from subhumid/humid to semi-arid regions is 30 times larger than that of the retreat from semi-arid to subhumid re-

**Table 2.** The contributions of different type transitions to the areal changes between 1948–62 and 1994–2008, units: $10^6$ km$^2$.

| Areas ($10^6$ km$^2$) | | | | |
|---|---|---|---|---|
| Arid to hyper-arid | Semi-arid to arid | Subhumid/humid to semi-arid | Humid to subhumid | Drier land |
| 0.049 | 0.084 | 0.638 | 0.606 | 1.377 |
| Hyper-arid to arid | Arid to semi-arid | Semi-arid to subhumid | Subhumid to humid | Wetter land |
| 0.114 | 0.092 | 0.021 | 0.047 | 0.274 |

gions. In addition, humid regions became drier and can even directly turn into semi-arid regions, which have contributed $0.087 \times 10^6$ km$^2$ to the expansion of semi-arid regions. All of these results indicate that aridity has intensified dramatically. Using the same method, the net expansions of arid and subhumid regions are $0.057 \times 10^6$ km$^2$ and $0.029 \times 10^6$ km$^2$, respectively.

### 3.2. *Climate change over drylands*

We also analyzed the climate variations over the expanded drylands according to the boundary of drylands for 1994–2008. The spatial distributions of trends of AI, SAT, precipitation and PET are shown in Fig. 5. AI shows a positive trend in the region to the west of 100°E and a negative trend to the east of 100°E (Fig. 5a). AI decreases significantly over the eastern drylands, and the trend rate of AI can reach $-0.06$ (10 yr)$^{-1}$ along the edge of drylands (e.g. in Hebei Province and northeast Inner Mongolia). This is the result of decreasing precipitation and increasing PET over the eastern drylands. The strong negative trend of AI in the east of northern China can lead to type transitions to drier types, like the transition from humid to subhumid, or even to semi-arid, thus further resulting in the expansion of drylands. Precipitation shows a "wet-west–dry-east" pattern over the expanded drylands, but even a slight increase in precipitation in the west cannot significantly mitigate the drought stress, and the decreasing trend can reach $-40$ mm (10 yr)$^{-1}$ in Hebei Province (Fig. 5c). The results are consistent with previous studies (Gong et al., 2004; Zhai et al., 2005; Zhang et al., 2011; Liu et al., 2013b; Wang et al., 2013a) that investigated the spatial and temporal variations of precipitation in China by using precipitation data from large amounts of meteorological stations. The temperature has increased during the past 61 years over most of the drylands, except for several small patches (Fig. 5b). Huang et al. (2012) examined SAT trends and found that the warming trend was particularly enhanced over semi-arid regions. Ji et al. (2014) further supported this result by using the spatiotemporal multidimensional ensemble empirical mode decomposition (MEEMD) method. In summary, the trend of aridity is enhanced in northern China, resulting from decreasing precipitation and increasing temperature in most of the areas in northern China, which leads to the expansion of drylands.

## 4. Summary and discussion

In this paper, we analyze the areal changes of drylands in terms of AI, and the regional climate variability in northern China, using historical records of SAT, precipitation and PET from 1948 to 2008. The results indicate that semi-arid regions dominate the coverage of drylands, which distribute in a northeast–northwest zonal band, covering most of Inner Mongolia, Hebei, Shanxi, northern Shaanxi, Ningxia, central Gansu, Qinghai and Tibet. The changes in precipitation patterns and increase of PET have led to an increase in aridity under global warming, and thus the expansion of drylands in northern China in the last 61 years. The total area of drylands of the last 15 years is $0.65 \times 10^6$ km$^2$ (12%) larger than

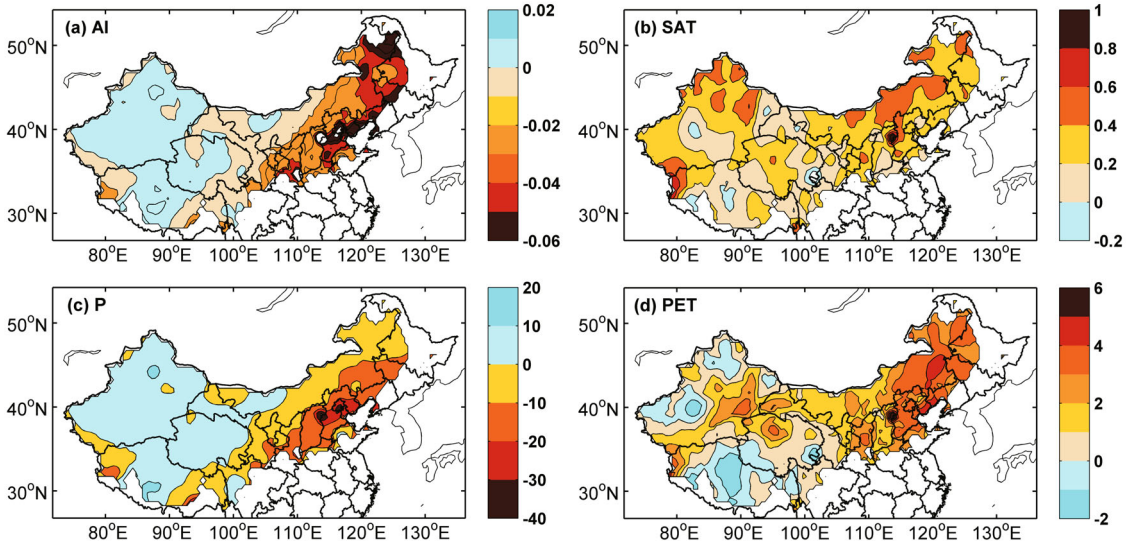


**Fig. 5.** Spatial distributions of trends of (a) AI [(10 yr)$^{-1}$], (b) SAT [°C (10 yr)$^{-1}$], (c) precipitation [mm (10 yr)$^{-1}$], and (d) PET [mm (10 yr)$^{-1}$] over the expanded drylands.

that in the period 1948–62. The areal change of drylands for 1994–2008 relative to 1948–62 shows a distinct boundary extension. The drylands over Northeast China have expanded nearly 2° of longitude to the east and 1° of latitude to the south along the middle-to-lower reaches of the Yellow River. Alongside the expansion, some regions have experienced dryland retreat. A major retreat of hyper-arid to arid regions has occurred on the edges of the Tarim Basin and Tianshan Mountains, and a retreat of arid to semi-arid regions has occurred mainly over central Tibet and on the edge of Junggar Basin. Among all the components of drylands, the expansion of semi-arid regions has played a dominant role in the areal extent of drylands, being nearly 10 times larger than those in arid and subhumid regions. In contrast, hyper-arid regions, which cover large areas of Xinjiang, some parts of Gansu, Qinghai and Tibet, and the northwestern edge of Inner Mongolia, shrank slightly from 1948 to 2008, at a rate of $-0.002 \times 10^6$ km$^2$ (10 yr)$^{-1}$. Therefore, we conclude that the total area of drylands in northern China has been expanding rapidly by $0.12 \times 10^6$ km$^2$ (10 yr)$^{-1}$, mainly driven by the rapid expansion of semi-arid regions.

The decrease of precipitation and increase of PET over eastern drylands under a warming climate have led to the increase in aridity and expansion of drylands in northern China. The precipitation in this region is strongly influenced by the summer monsoon, which is a major source of precipitation in China. A weakening of the summer monsoon, caused by changes in land cover (Fu and Yuan, 2001; Fu, 2003; Zhang et al., 2005), results in decreases in all the components of the surface water balance, such as precipitation, runoff, and soil water content. Wang and Li (1990) also found that a stronger Hadley circulation will induce a stronger intensity of the subtropical high, which in turn will lead to a decrease in the extent of the northern latitude of the summer monsoon and thus a decrease of precipitation in semi-arid regions in northern China. Temperature rises (Huang et al., 2012; Ji et al., 2014) lead to increased surface evaporation and a decrease in the surface water budget, which is unfavorable for water accumulation at the surface, and thus is an important factor causing aridity and dryland expansion. All these factors contribute to the expansion of drylands, but the individual contributions of these factors need to be clarified in further studies.

In summary, semi-arid regions are the most vulnerable and sensitive to regional climate change among all the four components of drylands. Although previous studies have already pointed out a significant expansion of global drylands, only a few studies have focused on northern China, which is a major region of arid and semi-arid land in East Asia. Therefore, further studies are needed to build upon the present study's findings to better understand the drylands of northern China.

***Acknowledgements.*** This work was jointly supported by the National Basic Research Program of China (Grant No. 2012CB 955301), the National Science Foundation of China (Grant Nos. 41175134 and 41305060), and a China 111 project (Grant No. B13045).

## REFERENCES

Agnew, C., and E. Anderson, 1992: *Water Resources in the Arid Realm*. Routledge, London, 323 pp.

Bi, J. R., J. P. Huang, F. Qiang, X. Wang, J. S. Shi, W. Zhang, Z. W. Huang, and B. D. Zhang, 2011: Toward characterization of the aerosol optical properties over Loess Plateau of Northwestern China. *Journal of Quantitative Spectroscopy and Radiative Transfer*, **112**, 346–360.

Chen, B., J. Huang, P. Minnis, Y. Hu, Y. Yi, Z. Liu, D. Zhang, and X. Wang, 2010: Detection of dust aerosol by combining CALIPSO active lidar and passive IIR measurements. *Atmos. Chem. Phys.*, **10**, 4241–4251.

Chen, M., P. Xie, J. E. Janowiak, and P. A. Arkuin, 2002: Global land precipitation: A 50-yr monthly analysis based on gauge observations. *Journal of Hydrometeorology*, **3**, 249–266.

Chen, S. Y., J. P. Huang, C. Zhao, Y. Qian, L. R. Leung, and B. Yang, 2013: Modeling the transport and radiative forcing of Taklimakan dust over the Tibetan Plateau: A case study in the summer of 2006. *J. Geophys. Res.*, **118**, 797–812.

Dai, A. G., 2011: Characteristics and trends in various forms of the Palmer drought severity index during 1900–2008. *J. Geophys. Res.*, **116**(D12115), doi: 10.1029/2010JD015541.

Dai, A. G., 2013: Increasing drought under global warming in observations and models. *Nature Climate Change*, **3**, 52–58.

Dietz, A. J., R. Ruben, and A. Verhagen, 2004: *The Impact of Climate Change on Drylands*. Springer, 465 pp.

Donohue, R. J., T. R. McVicar, and M. L. Roderick, 2010: Assessing the ability of potential evaporation formulations to capture the dynamics in evaporative demand within a changing climate. *J. Hydrol.*, **386**, 186–197.

Fan, Y., and H. van den Dool, 2008: A global monthly land surface air temperature analysis for 1984-present. *J. Geophys. Res.*, **113**(D01103), doi: 10.1029/2007JD008470.

Feng, S., and Q. Fu, 2013: Expansion of global drylands under a warming climate. *Atmos. Chem. Phys.*, **13**, 10081–10094.

Fu, C., 2003: Potential impacts of human-induced land cover change on East Asia monsoon. *Global Planetary Change*, **37**, 219–229.

Fu, C., Z. Jiang, Z. Guan, J. He, and Z. Xu, 2008: *Regional Climate Studies of China*. Springer, 476 pp.

Fu, C. B., and H. L. Yuan, 2001: An virtual numerical experiment to understand the impacts of recovering natural vegetation on the summer climate and environmental conditions in East Asia. *Chinese Science Bulletin*, **46**, 1199–1203.

GLP, 2005: Global Land Project—Science plan and implementation strategy. IGBP (International Geosphere Biosphere Program) Report No. 53/International Human Dimensions Programme Report No.19, IGBP Secretariat, Stockholm, 64 pp.

Gong, D. Y., P. J. Shi, and J. A. Wang, 2004: Daily precipitation changes in the semi-arid region over northern China. *Journal of Arid Environments*, **59**, 771–784.

Huang, J., P. Minnis, H. Yan, Y. Yi, B. Chen, L. Zhang, and J. K. Ayers, 2010: Dust aerosol effect on semi-arid climate over Northwest China detected from A-Train satellite measurements. *Atmos. Chem. Phys.*, **10**, 6863–6872.

Huang, J., X. Guan, and F. Ji, 2012: Enhanced cold-season warming in semi-arid regions. *Atmos. Chem. Phys.*, **12**, 5391–5398.

Huang, J. P., 2013: Observing the impact of Asia dust aerosols on aridity. *SPIE Newsroom*, doi: 10.1117/2.1201306.004858.

Huang, J. P., J. M. Ge, and F. Z. Weng, 2007: Detection of Asia dust storms using multisensor satellite measurements. *Remote*

*Sensing of Environment*, **110**, 186–191.

Huang, J. P., and Coauthors, 2008: An overview of the semi-arid climate and environment research observatory over the Loess Plateau. *Adv. Atmos. Sci.*, **25**, 906–9211, doi: 10.1007/s00376-008-0906-7.

Hulme, M., 1996: Recent climatic change in the world's drylands. *Geophys. Res. Lett.*, **23**, 61–64.

Ji, F., Z. H. Wu, J. P. Huang, and E. P. Chassignet, 2014: Evolution of land surface air temperature trend. *Nature Climate Change*, **4**, 462–466, doi: 10.1038/nclimate2223.

Liu, L., X. L. Xu, D. F. Zhuang, X. Chen, and S. Li, 2013a: Changes in the potential multiple cropping system in response to climate change in China from 1960–2010. *Plos One*, **8**(12), e80990.

Liu, X. M., D. Zhang, Y. Z. Luo, and C. M. Liu, 2013b: Spatial and temporal changes in aridity index in northwest China: 1960 to 2010. *Theor. Appl. Climatol.*, **112**, 307–316.

Ma, Z. G., and C. B. Fu, 2003: Interannual characteristics of the surface hydrological variables over the arid and semi-arid areas of northern China. *Global Planetary Change*, **37**, 189–200.

Ma, Z. G., and L. Dan, 2005: Dry/wet variation and its relationship with regional warming in arid-regions of Northern China. *Chinese Journal of Geophysics*, **48**, 1091–1099.

Ma, Z. G., and C. B. Fu, 2006: Some evidence of drying trend over northern China from 1951 to 2004. *Chinese Science Bulletin*, **51**, 2913–2925.

Ma, Z. G., and C. B. Fu, 2007: Global aridification in the second half of the 20th century and its relationship to large-scale climate background. *Science in China Series D: Earth Sciences*, **50**, 776–788.

Ma, Z. G., C. B. Fu, and L. Dan, 2005: Decadal variations of arid and semi-arid boundary in China. *Chinese Journal of Geophysics*, **48**, 574–581.

Maidment, D. R., 1993: *Handbook of Hydrology*. McGraw-Hill, 1424 pp.

Middleton, N. J., and D. S. G. Thomas, 1997: *World Atlas of Desertification*. 2nd ed., Edward Arnold, 182 pp.

Millennium Ecosystem Assessment, 2005: *Ecosystems and Human Well-being: Synthesis*. Island Press, Washington, DC., 137 pp.

Mortimore, M., 2009: *Dryland Opportunities*. Island Press, 98 pp.

Nicholson, S. E., 2011: *Dryland Climatology*. Cambridge University Press, 516 pp.

Overpeck, J., and B. Udall, 2010: Dry times ahead. *Science*, **328**, 1642–1643.

Reed, S. C., K. K. Coe, J. P. Sparks, D. C. Housman, T. J. Zelikova, and J. Belnap, 2012: Changes to dryland rainfall result in rapid moss mortality and altered soil fertility. *Nature Climate Change*, **2**, 752–755.

Reynolds, J. F., and Coauthors, 2007: Global desertification: building a science for dryland development. *Science*, **316**, 847–851.

Rodell, M., and Coauthors, 2004: The global land data assimilation system. *Bull. Amer. Meteor. Soc.*, **85**, 381–394.

Safriel, U., and Z. Adeel, 2005: Dryland systems. *Ecosystems and Human Well-being, Current State and Trends*, Hassan et al., Eds., Island Press, Washington, 625–658.

Seager, R., and Coauthors, 2007: Model projections of an imminent transition to a more arid climate in southwestern North America. *Science*, **316**, 1181–1184.

Stadler, S. J., 2005: Aridity indices, 89–94. *Encyclopedia of World Climatology*, Oliver et al., Eds., Heidelberg. Springer, 854 pp.

Sun, W., 2000: Interaction between desertification boundary and pressure lines of population and husbandry in the Houshan area of Bashang since 1950. *Journal of Desert Research*, **20**, 154–158 (in Chinese).

UNCCD, 1994: United Nations Convention to Combat Desertification in Those Countries Experiencing Serious Drought and/or Desertification, Particularly in Africa (UNCCD). U.N. Doc. A/AC.241/27, 33 I.L.M. 1328, United Nations, 58 pp. [Available online at http://www.unccd.int/Lists/SiteDocumentLibrary/conventionText/conv-eng.pdf.]

Wang, H. J., Y. N. Chen, and Z. S. Chen, 2013a: Spatial distribution and temporal trends of mean precipitation and extremes in the arid region, northwest of China, during 1960–2010. *Hydrological Processes*, **27**, 1807–1818.

Wang, T., W. Wu, X. Xue, W. M. Zhang, Z. W. Han, and Q. W. Sun, 2003: Time-space evolution of desertification land in northern China. *Journal of Desert Research*, **23**, 230–235 (in Chinese).

Wang, W. C., and K. R. Li, 1990: Precipitation fluctuation over semiarid region in Northern China and the relationship with El Niño/Southern oscillation. *J. Climate*, **3**, 769–783.

Wang, X. M., F. H. Chen, and Z. B. Dong, 2006: The relative role of climatic and human factors in desertification in semiarid China. *Global Environmental Change*, **16**, 48–57.

Wang, X., J. Huang, M. Ji, and K. Higuchi, 2008: Variability of East Asia dust events and their long-term trend. *Atmos. Environ.*, **42**, 3156–3165.

Wang, X., J. P. Huang, R. D. Zhang, B. Chen, and J. R. Bi, 2010: Surface measurements of aerosol properties over northwest China during ARM China 2008 deployment. *J. Geophys. Res.*, **115**(D7), doi: 10.1029/2009JD013467.

Wang, X., S. J. Doherty, and J. P. Huang, 2013b: Black carbon and other light-absorbing impurities in snow across Northern China. *J. Geophys. Res.*, **118**, 1471–1492.

Wang, X., B. Q. Xu, and J. Ming, 2014: An overview of the studies on black carbon and mineral dust deposited in snow and ice core in East Asia. *J. Meteor. Res.*, **28**, 354–370.

Xi, X., and I. N. Sokolik, 2012: Impact of Asian dust aerosol and surface albedo on photosynthetically active radiation and surface radiative balance in dryland ecosystems. *Advances in Meteorology*, **2012**, Article ID 276207, doi: 10.1155/2012/276207.

Yang, X., K. Zhang, B. Jia, and L. Ci, 2005: Desertification assessment in China: An overview. *Journal of Arid Environments*, **63**, 517–531.

Zhai, P. M., X. B. Zhang, H. Wan, and X. H. Pan, 2005: Trends in total precipitation and frequency of daily precipitation extremes over China. *J. Climate*, **18**, 1096–1108.

Zhang, J. Y., W. J. Dong, and C. B. Fu, 2005: Impact of land surface degradation in northern China and southern Mongolia on regional climate. *Chinese Science Bulletin*, **50**, 75–81.

Zhang, Q., C. Y. Xu, X. H. Chen, and Z. X. Zhang, 2011: Statistical behaviours of precipitation regimes in China and their links with atmospheric circulation 1960–2005. *International Journal of Climatology*, **31**, 1665–1678.